Available online at www.sciencedirect.com
ScienceDirect
Journal of Nuclear Materials 367–370 (2007) 423–427
journal of nuclear materials
www.elsevier.com/locate/jnucmat

Evaluation of Helium effects on swelling behavior of oxide dispersion strengthened ferritic steels under ion irradiation

K. Yutani [a], H. Kishimoto [b], R. Kasada [b], A. Kimura [b,*]

[a] *Graduate School of Energy Science, Kyoto University, Gokasho, Uji, Kyoto 611-0011, Japan*
[b] *Institute of Advanced Energy, Kyoto University, Gokasho, Uji, Kyoto 611-0011, Japan*

Abstract

Effects of ion-irradiation on the swelling behavior were investigated for a high-chromium oxide dispersion strengthened (ODS) ferritic steel and a 9Cr–2W reduced-activation ferritic (RAF) steel up to a high dose (nominal 60 dpa) with and without helium (900 appm) by using single and dual-ion irradiation techniques at 773 K. Microstructure observations revealed that the average size and number density of cavities formed in the ODS steel are half the size and twice the density of those in the RAF steel, indicating that the ODS steel has superior resistance to swelling. Trapping of helium atoms and vacancies at the boundaries between the nano-sized oxide particles and the matrix probably accelerated nucleation of bubbles and prevented the voids from growing. It is concluded that small oxide particles in high density are effective traps for helium atoms and/or vacancies by offering a high number density of trapping sites.

1. Introduction

Oxide dispersion strengthened (ODS) ferritic steels have received considerable attentions because of superior characteristics in high-temperature and high-dose neutron irradiation environments in fast breeder reactors (FBRs) and fusion reactors. The 9Cr ODS steels developed as fuel cladding for sodium-cooled FBRs showed excellent high-temperature strength resulting from nano-sized oxide particle dispersions [1,2]. Furthermore, our research group has developed high-chromium ODS steels to increase corrosion resistance in super critical pressurized water, which is envisaged to be used for the advanced fission and fusion reactor systems [3–7]. As for irradiation effects in the ODS steels, swelling behavior under neutron irradiation was partly investigated [8], but there were few studies concerning effects of transmutation helium on swelling [9]. Since there are no operating fusion reactor or intense fusion spectrum neutron source such as the International Fusion Material Irradiation Facility (IFMIF) available, most of the studies on fusion materials rely on simulation experiments by means of isotopic- and spectral-tailoring methods to examine synergistic effects of atomic-displacement damage and helium production by (n, α) nuclear transmutations [10]. However, the additional Ni or B elements used in these methods directly affect the swelling behavior [11] and mechanical properties [12]. The Dual-ion irradiation technique is an effective methods to simulate fusion neutron irradiation

* Corresponding author. Tel.: +81 774 38 3483; fax: +81 774 38 3479.
E-mail address: kimura@iae.kyoto-u.ac.jp (A. Kimura).

0022-3115/$ - see front matter © 2007 Elsevier B.V. All rights reserved.
doi:10.1016/j.jnucmat.2007.03.016

because no additional elements are used [13]. In particular, the DuET facility allows variable irradiation conditions and high doses with precise current monitoring and temperature control [14].

The objective of this study is to investigate the effects of helium on the swelling behavior of ODS steels up to high dose using a dual-ion irradiation facility.

2. Experimental procedure

The materials used in this study were a high-chromium (16Cr–4.5Al) ODS steel designated K3-ODS steel and JLF-1 RAF steel. The chemical compositions and heat treatment conditions are given in Table 1. Specimen surfaces for ion irradiation were mechanically polished using 0.3 μm alumina abrasive particles, followed by electro-polishing in a solution of 5 vol.% perchloric acid +95 vol.% methanol to remove the damaged surface layer resulting from mechanical polishing.

Dual-ion irradiation, using 6.4 MeV Fe^{3+} ions for displacement damage simultaneously with energy-degraded 1.0 MeV He^{+} ions, was carried out using the DuET facility at the Institute of Advanced Energy, Kyoto University. Single-ion irradiations used 6.4 MeV Fe^{3+}. The irradiation temperature was controlled at $773\,K \pm 5\,K$ by monitoring the temperature of the specimen surface using infrared thermography during irradiation. The nominal conditions for ion irradiations, at 600 nm below the specimen surface, were calculated by TRIM-98 code, and are as follows: dose rate: 1×10^{-3} dpa/s, dose:nominal damage 60 dpa, helium to dpa ratio: 15 appm He/dpa. The displacement damage at the peak position is estimated to be 150 dpa.

Thin foils (10 μm × 10 μm × < 0.1 μm) for transmission electron microscopy (TEM) were prepared by the focused ion beam (FIB) method, in order to observe a limited ion irradiation range and to minimize the effect of ferromagnetism. Finally, flash electro-polishing was used to remove the surface layer damaged by FIB. The foil was lifted using a micro pick-up system and mounted onto a collodion film supported by copper mesh, and anchored by vapor deposited carbon. The thin foils were observed with a JEM-2010 TEM operated at 200 kV. A convergent-beam electron diffraction technique was used for measuring the thickness of the TEM specimen. The observed area was estimated to be a dual-ion irradiated region about 500–1200 nm below from the irradiated surface, based on the TRIM-98 code calculation.

3. Results

Fig. 1 shows typical TEM images of (a) single-ion, (b) dual-ion irradiated K3-ODS steel, and (c) single-ion, (d) dual-ion irradiated JLF-1 steel, respectively, in regions irradiated up to 60 dpa with 900 appm implanted helium. All specimens were irradiated at 773 K. The TEM images were obtained from cross sectional specimens prepared by the FIB method. The images shown in Fig. 1 were taken at 600–900 nm depth from the irradiated surface. The single-ion irradiation has no visible effects on the microstructure of K3-ODS and JLF-1 steels, as can be seen in Fig. 1(a) and (c). The fine black dots observed in Fig. 1(a) and (b) were identified as oxide particles, and are also observed in unirradiated material [15]. In contrast, dual-ion irradiation of the K3-ODS steel gave rise to the formation of a very high concentration of tiny cavities in the matrix as well as at matrix/oxide interfaces. The observed tiny cavities seem to be helium gas filled bubbles because the shape of the cavities is spherical. For the dual-ion irradiated JLF-1 steel, a significant change in the microstructure was also observed, as shown in Fig. 1(d). The cavities formed in the JLF-1 steel are much larger than in the K3-ODS steel irradiated to the same condition. Furthermore, some of the large cavities in the JLF-1 steel show faceted shapes.

Fig. 2 shows the average diameter and number density of cavities observed in the dual-ion irradi-

Table 1
Chemical composition and heat treatment conditions of the steels used in the experiment

(wt%)

ID	C	Cr	W	Al	Ti	V	Ta	Si	P	S	Mn	N	Y_2O_3
K3[a]	0.08	16.00	1.82	4.59	0.28	–	–	0.033	<0.005	0.002	0.06	0.006	0.368
JLF-1[b]	0.097	9.04	1.97	0.003	–	0.19	0.07	<0.1	0.003	0.002	0.46	0.0237	–

[a] Hot extrusion at 1423 K after Mechanical Alloying and tempered at 1323 K × 3.6 ks followed by air-cooling.
[b] Normalized at 1323 K 3.6 ks followed by air-cooling and tempered at 1053 K × 3.6 ks followed by air-cooling.

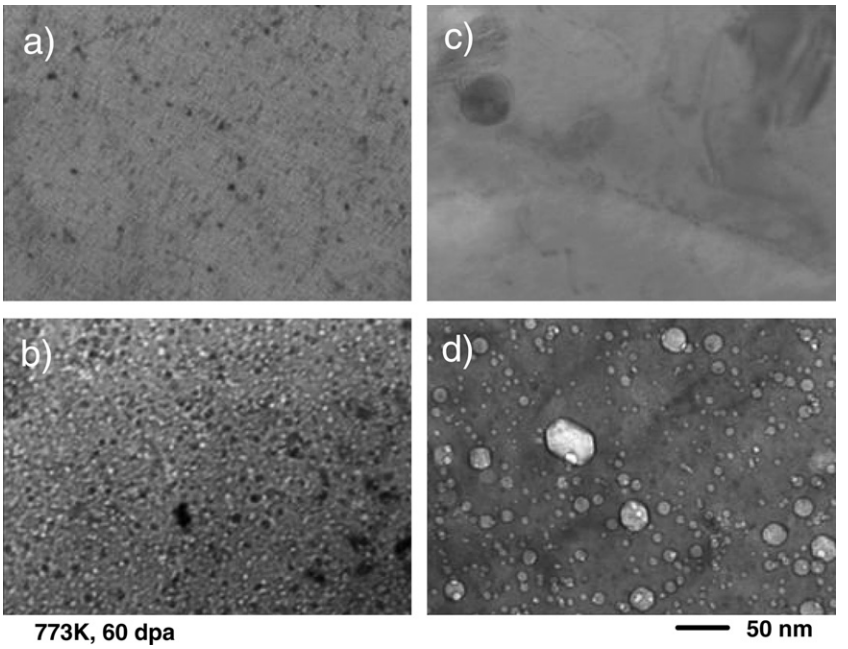

Fig. 1. TEM images of the (a) single-ion and (b) dual-ion irradiated K3-ODS steel, and of the (c) single- and (d) dual-ion irradiated JLF-1 steel at 773 K and 60 dpa.

ated K3-ODS steel and JLF-1 steel, which are plotted against displacement damage (dpa) calculated from the TRIM-98 code. It can be seen that the increase in average diameter with increasing displacement damage is smaller for the ODS steel than for the JLF-1 steel. On the other hand, the cavity number density in the K3-ODS steel is higher than in the JLF-1 steel, even at low dpa. Fig. 3 shows the size distributions of cavities formed in the dual-ion irradiated K3-ODS steel and JLF-1 steel at a depth of about 800 nm from the irradiated surface. It can be stated that the growth rate of cavities in the K3-ODS steel is significantly higher than in the JLF-1 steel. Smaller cavities (<5 nm dia), probably helium bubbles, exist in the K3-ODS in much higher density than in the JLF-1 steel. On the other

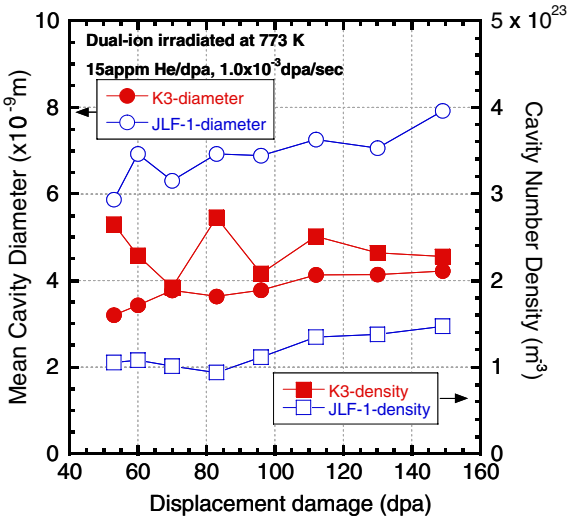

Fig. 2. Mean cavity diameter and cavity number density versus displacement damage for the K3-ODS and JLF-1 steels.

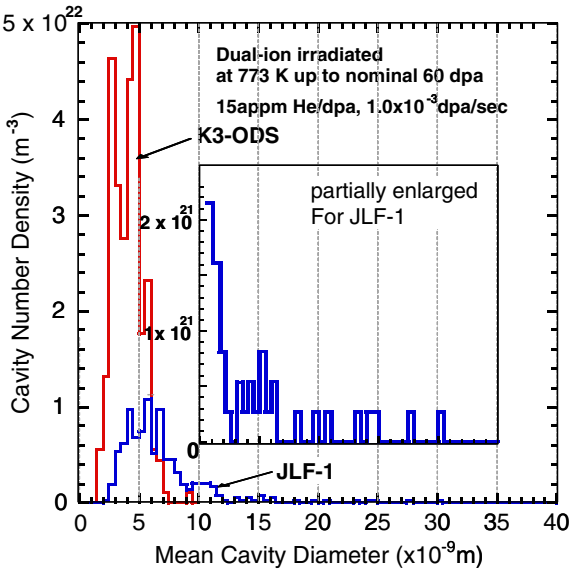

Fig. 3. Size distributions of cavities formed in the dual-ion irradiated K3-ODS and JLF-1 steels.

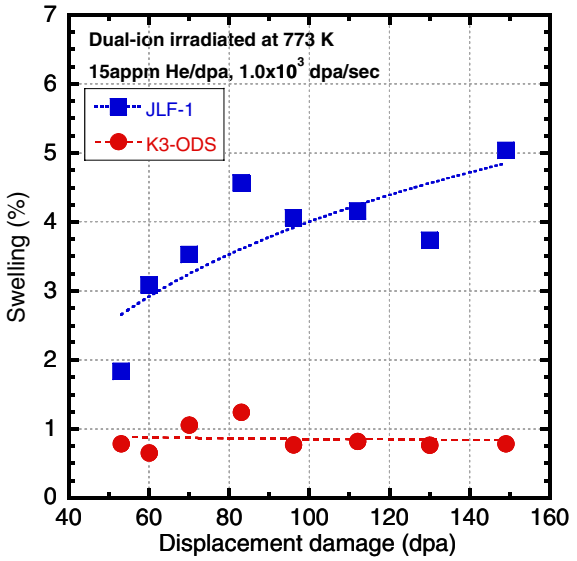

Fig. 4. Swelling versus displacement damage for the K3-ODS and JLF-1 steels.

hand, the expected bi-modal distribution, which consists of smaller helium bubbles and larger voids (diameter between 10 and 40 nm), was confirmed in the dual-ion irradiated JLF-1 steel.

Fig. 4 shows the swelling vs displacement damage (dpa) profile, calculated from the cavity diameter and number density estimated from the data shown in Fig. 2 for a given volume of observed area. The amount of swelling of the K3-ODS steel is significantly lower than that of the JLF-1 steel up to the higher dose region (about 150 dpa). While the swelling value of the JLF-1 steel increases with the displacement damage, that of the K3-ODS steel remains constant.

4. Discussion

The single-ion irradiated K3-ODS steel shows no detectable change, as shown in Fig. 1(a). Gelles investigated the swelling behavior of the commercial ODS steel MA956 (19Cr–4.2Al–0.34Ti–0.48Y_2O_3) irradiated up to about 200 dpa at 693 K in the FFTF reactor [16], where the amount of transmutation helium is very low because of the neutron spectrum. The MA956 showed an extremely low void swelling value, which was estimated to be about 1.17% from density change measurements, and estimated to be 0.21% from TEM observations. Although the values estimated by each method are different, the swelling of MA956 was small. An excellent resistance to the high dose neutron irradiation was also observed for the K3-ODS steel irradiated with iron ions up to 150 dpa, with simultaneous helium implantation, as shown in Fig. 4.

The swelling of the K3-ODS steel was lower than that of the JLF-1 steel and nearly constant vs. displacement damage, as shown in Fig. 4. This behavior can be attributed to the higher number density and smaller size of cavities in the K3-ODS steel. Even in the lower dose region, the cavity number density is high, indicating that the K3-ODS steel has specific trapping sites for helium atoms and vacancies, so that cavity nucleation at the early stage of irradiation is enhanced and limits subsequent cavity growth. It is expected that nano-sized oxide particles dispersed in the fine grains of the K3-ODS steel have a significant influence on the nucleation and growth processes of cavities. Fig. 5 shows TEM images of (a) a cavity, probably an argon bubble formed during mechanical alloying [17], which is adjacent to an oxide particle in the as-received K3-ODS steel, and (b) cavities adjacent to oxide particles in the dual-ion irradiated K3-ODS steel, suggesting that the interface between oxide particle and matrix is suitable for trapping gas atoms, including both helium and argon. However, the number density of oxide particles (estimated by TEM as 1.3×10^{22} m^{-3}) is one order of magnitude lower than that of cavities (estimated by TEM as 2.2×10^{23} m^{-3}). While the oxide particles are distinctly effective trapping sites for helium and vacancies, finer particles below the TEM resolution limit should also exist as trapping sites to explain the suppression of swelling in the ODS steel. Two types of very fine trapping sites may exist: very fine nano-sized oxide particles, invisible because of the TEM resolution limit, and invisible α' phase particles that form in high chromium ferritic steels under irradiation. The presence of very fine oxides was suggested by small angular neutron scattering measurements [18]. The effects of chromium concentration on swelling of Fe–Cr binary ferritic alloys irradiated to high neutron fluence in FFTF/MOTA indicated that the amount of swelling decreases with increasing chromium concentration above 9 wt% [19]. Another possible interpretation is a reduction of helium concentration at grain boundaries because of high density of grain boundaries in fine grain of the ODS steel. Further investigation is needed to clarify the swelling mechanism in high-chromium ODS steels.

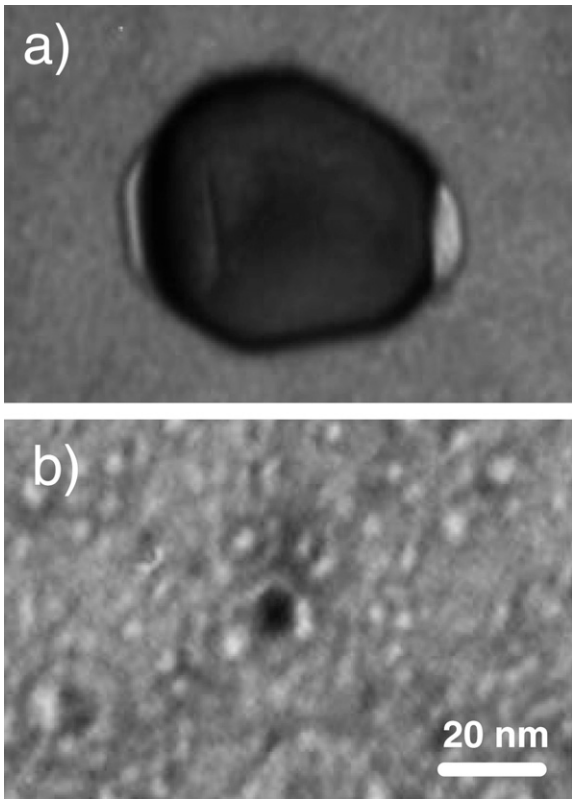

Fig. 5. TEM images of (a) argon and (b) helium bubbles at oxide particles in the K3-ODS steel.

5. Conclusions

Synergistic effects of irradiation displacement damage and helium atoms on the microstructural evolution of the K3-ODS steel and the JLF-1 RAF steel were investigated using a dual-ion irradiation technique:

(1) A high density of fine helium bubbles (<5 nm dia) was observed in the K3-ODS steel after dual-ion irradiation at 773 K to nominal 60 dpa. In contrast, no cavities were observed after single-ion irradiation.
(2) Microstructure observations revealed that the average size and number density of cavities formed in the ODS steels ware half the size and twice the density of those in the JLF-1 RAF steel, indicating that the ODS steels has superior resistance to swelling. Bi-modal distribution consisting of coarsened voids and tiny bubbles was confirmed to form in the JLF-1 RAF steel.
(3) The experimental results demonstrated that the K3-ODS steel has superior resistance to swelling under dual-ion irradiation up to a dose of about 150 dpa, as compared to the JLF-1 RAF steel. It is believed that suppression of the growth of cavities in the ODS steel is due to the existence of trapping sites in higher density. These may be nano-sized oxide particles whose small size is below the TEM resolution limit, and/or α' phase formed during irradiation.

Acknowledgements

The authors thank O. Hashitomi, H. Ogiwara and K. Ozawa for help with the DuET facility. The authors also thank T. Omura for help in using the FIB and TEM.

References

[1] S. Ukai, M. Harada, H. Okada, M. Inoue, S. Nomura, S. Shikakura, T. Nishida, M. Fujiwara, K. Asabe, J. Nucl. Mater. 204 (1993) 74.
[2] S. Ukai, T. Okuda, M. Fujiwara, T. Kobayashi, S. Mizuta, H. Nakashima, J. Nucl. Sci. Technol. 39(8), 872.
[3] H.S. Cho, A. Kimura, S. Ukai, M. Fujiwara, J. Nucl. Sci. Technol. 329–333 (2004) 387.
[4] J.S. Lee, A. Kimura, S. Ukai, M. Fujiwara, J. Nucl. Mater. 329–333 (2004) 1122.
[5] N.Y. Iwata, A. Kimura, S. Ukai, M. Fujiwara, N. Kawashima, in: Proc. of ICAPP '05, Seoul, KOREA, 2005, 5528.
[6] H. Kishimoto, K. Yutani, R. Kasada, A. Kimura, in: Proc. of ICAPP '05, Seoul, KOREA, 2005, 5465.
[7] A. Kimura, H.S. Cho, S. Ukai, M. Fujiwara, in: Proc. of ICAPP '04, Pittsburgh, PA, USA, 2004, 2070.
[8] M.B. Toloczko, D.S. Gelles, F.A. Garner, R.J. Kurtz, K. Abe, J. Nucl. Mater. 329–333 (2004) 352.
[9] S. Yamashita, S. Watanabe, S. Ohnuki, H. Takahashi, N. Akasaka, S. Ukai, J. Nucl. Mater. 283–287 (2000) 647.
[10] N. Hashimoto, R.L. Klueh, J. Nucl. Mater. 305 (2002) 153.
[11] T. Morimura, A. Kimura, H. Matsui, J. Nucl. Mater. 239 (1996) 118.
[12] R. Kasada, A. Kimura, Mater. Trans. 46 (2005) 475.
[13] H. Ogiwara, H. Sakasegawa, H. Tanigawa, M. Ando, Y. Katoh, A. Kohyama, J. Nucl Mater. 307–311 (2002) 299.
[14] A. Kohyama, Y. Katoh, M. Ando, K. Jimbo, Fus. Eng. Des. 51–52 (2000) 789.
[15] R. Kasada, N. Toda, H.S. Cho, A. Kimura, Proc. of ICAPP '05, Seoul, KOREA, 2005, 5328.
[16] D.S. Gelles, J. Nucl. Mater. 233–237 (1996) 293.
[17] M. Klimiankou, R. Lindau, A. Moslang, Micron 36 (2005) 1.
[18] M.J. Alinger, G.R. Odette, D.T. Hoelzer, J. Nucl. Mater. 329–333 (2004) 382.
[19] Y. Katoh, A. Kohyama, D.S. Gelles, J. Nucl. Mater. 225 (1995) 154.